

Microphase Separation in Comb Copolymers

Aritomo Shinozaki,^{*,†} David Jasnow,[‡] and Anna C. Balazs[†]

Department of Materials Science and Engineering and Department of Physics and Astronomy, University of Pittsburgh, Pittsburgh, Pennsylvania 15260

Received November 11, 1993; Revised Manuscript Received February 7, 1994*

ABSTRACT: Microphase separation in comblike copolymers, in which the backbone is of one monomeric species and the teeth are of another species, is discussed. Within the random phase approximation of Leibler, we calculate the spinodal transition curve (χN), as a function of compositional fraction f of backbone monomers. The comb is assumed to have either evenly spaced grafting points or randomly placed grafting points. The evenly spaced copolymers have teeth symmetrically or asymmetrically placed on the backbone. In the evenly spaced copolymer melt, as the number of teeth (n_t) is increased in the comb, the spinodal curve changes toward a fixed form. The spinodal curves approach the large- n_t form as a function of n_t from significantly different directions depending on the symmetry. This difference led us to consider the consequence of random placement of the teeth. The copolymer melt with randomly placed teeth approaches a significantly different spinodal curve in the limit of large n_t . More importantly, the scaling of the instability wave vector in the limit of large n_t changes from the expected $q^* \sim (n_t/N)^{1/2}$ to $q^* \sim (n_t^{1/4}/N^{1/2})$. These results call into question the assumption of well-ordered comb copolymers as a basis for computing detailed properties of melts.

I. Introduction

The behavior of diblock copolymers has sparked considerable interest and has been the subject of numerous experimental and theoretical investigations. The reason for this interest arises from the fact that diblocks can be composed of two incompatible polymers. When the repulsion between these fragments is sufficiently high, the melt will attempt to undergo phase separation; however, since the incompatible blocks are chemically linked, the system can only exhibit microphase separation. This type of microphase separation can occur in other chain morphologies that contain incompatible segments. Of particular interest is determining the phase behavior of comb copolymers, macromolecules that contain a backbone and "teeth" or "branches" that emanate from the backbone. This task is particularly important since commercially synthesized copolymers frequently display some degree of branching. To make effective predictions concerning the behavior of these melts, the presence of the branches must be taken into account. Furthermore, since there are more junction points in a comb than a diblock, investigations into the properties of combs may reveal novel phase behavior.

In this paper, we use a mean-field theory of the type developed by Leibler¹ (and generalized by Ohta and Kawasaki²) to examine the phase behavior of a melt of AB comb copolymers, where the backbones are composed of a flexible A segment and the flexible teeth are composed of B monomers. In this study, we only consider the stability of the homogeneous phase relative to the microphase-separated state. In particular, we calculate the spinodal curve in terms of the normalized Flory–Huggins parameter χN , the relative AB composition, and n_t , the number of teeth in the comb.

In previous studies, Olvera de la Cruz and Sanchez³ determined the spinodal for a melt of AB combs with a single tooth. Benoit and Hadziioannou⁴ calculated this curve for a melt of uniform combs in which the teeth are spaced at regular intervals along the length of the backbone. These teeth, however, were not centered about

the midpoint of the backbone but were placed in an asymmetric pattern, as shown schematically in Figure 1A. To initiate our studies, we considered a melt of uniform combs in which the teeth are symmetrically placed along the backbone, as shown in Figure 1B. As we demonstrate below, this simple deviation in architecture yields pronounced changes in the phase behavior for modest numbers of teeth.

These findings lead us to consider the effect of "architectural dispersity". That is, we consider a melt of combs in which the copolymers are not identical and the teeth are randomly distributed along the length of the backbone (see Figure 1C). We emphasize that we consider the case with monodisperse length teeth and backbones. The only difference from polymer to polymer in the melt is in the placement of the teeth on the backbone. When compared to the melt of uniform chains with regularly spaced teeth, such architectural dispersity leads to significantly different phase behavior. Since actual melts more closely resemble this architecturally disperse case, our findings can provide insight into the behavior of systems of experimental interest.

II. Theoretical Approach

In this short paper, we will only be concerned with the boundary of the thermodynamic instability of the homogeneous phase to a microphase-separated phase. This transition is quite generally preempted by a first-order transition. However, a full mean-field calculation of the first-order transition and region of metastability would require the computation of at least the fourth-order terms in the coarse-grained free energy.

If we restrict our attention to the spinodal instability, we need only concentrate on the second-order term, which is a great simplification. Calculation of higher order terms would also be necessary in studying the possible equilibrium morphologies of the microphase-separated domains, at least in the weak-segregation regime. We reserve this for later study. Finally, we only consider mean-field theory and expect that a more detailed calculation involving fluctuations about mean-field theory^{5–7} will exhibit interesting corrections.

We assume that the length in monomer units of the A backbone chain is N_A . The length of each B tooth is N_B ,

[†] Department of Materials Science and Engineering.

[‡] Department of Physics and Astronomy.

* Abstract published in *Advance ACS Abstracts*, March 15, 1994.

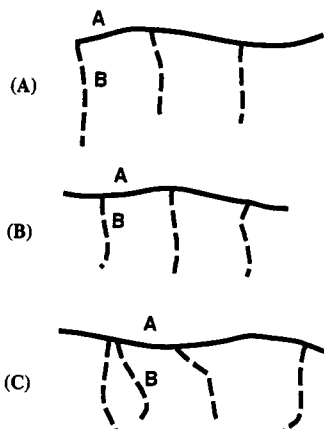


Figure 1. (A) Caricature of an asymmetric, evenly spaced comb copolymer with 3 teeth. The main chain consists of monomers of species A, and the chains comprising the teeth consist of species B. (B) Caricature of a symmetric comb copolymer with 3 teeth. (C) Caricature of a comb copolymer with 4 randomly placed teeth.

while the number of teeth is denoted by n_t . We assume that the A and B monomers are of the same size. In the symmetric and asymmetric comb copolymers, we also assume that the placement of the teeth is ideal. This means that the distance between teeth is N_A/n_t , and the distance from the beginning of the A chain to the first tooth is tN_A/n_t , with $t = 0$ in the asymmetric case and $t = 1/2$ in the symmetric case. Of course, any $0 \leq t \leq 1/2$ is possible, but we will concentrate on the two extreme examples. In the comb copolymer with randomly placed teeth, we will assume the same number of teeth n_t in each copolymer but that the position of each tooth is random, with uniform probability of the tooth being attached anywhere on the backbone. In all cases, the total number of monomers in the polymer is $N = N_A + n_t N_B$, while the relative fraction of A (backbone) monomers is $f = f_A = N_A/N$. Likewise $f_B = 1 - f_A$. Finally, we define for future use $f_{At} = f_A/n_t$ and $f_{Bt} = f_B/n_t$.

In the Hamiltonian for the system, the chains are assumed to be Gaussian when χ , the Flory-Huggins interaction energy, equals zero. For a comb copolymer with closely spaced teeth, the assumption of Gaussian statistics, even at $\chi = 0$, may not be highly realistic. Such chains may be stretched relative to the Gaussian case, even in the homogeneous melt. For evenly spaced teeth, one can make a crude estimate of the applicability of Gaussian statistics. We will consider the linear size of monomers to be normalized to unity and estimate the monomer density due to a single Gaussian chain comb. If the monomer density ρ is sufficiently small, the teeth of a single polymer do not significantly interfere with each other, and the Gaussian assumption is reasonable.

Briefly consider the average monomer density ρ_R within a region radius R about a fixed end point of a Gaussian chain. The number of monomers within the region is roughly $N \sim R^2$. Hence $\rho_R \sim N/R^3 \sim 1/R$. Now consider the junction point of a tooth and the backbone. We assume that the length of the tooth N_t is much less than the length of the backbone N_b . For $R < N_t^{1/2}$, we would then have $\rho_R \sim 3/R$, where we account for the tooth and the two stretches of backbone emanating from the junction point. Near the junction point, it is possible for the density to be large. However, at the length scale of the tooth, $\rho \sim 3/N_t^{1/2}$. If $N_t^{1/2}$ is sufficiently large, one expects this contribution to the density to be less than unity.

Now we must account for the effect of the other teeth. Let M be the number of monomers between attachment points of teeth along the backbone. Consider a given tooth and the distance of its attachment point on the backbone

to the attachment points of the other teeth. The nearest and next-nearest pair of teeth are attached $M^{1/2}$ and $(2M)^{1/2}$ away from the given tooth. Likewise, the n th pair, which we assume is at a radius of gyration away from the given tooth, obeys $(nM)^{1/2} \sim N_t^{1/2}$. Hence, the number of teeth overlapping the attachment point of a given tooth is given by $n \sim N_t/M$.

The contribution to the monomer density by the nearest pair of teeth about a given tooth is roughly $2/M^{1/2}$. The next pair contributes roughly $2/(2M)^{1/2}$ and so on. Thus $\rho_{\text{other}} \sim 2 \sum_{n=1}^{N_t/M} [1/(nM)^{1/2}]$. One can estimate the sum to be $4N_t^{1/2}/M$. Thus the monomer density in the vicinity of a given tooth is $\rho \sim 3/N_t^{1/2} + 4N_t^{1/2}/M$. Hence, we can ensure ρ is sufficiently small if, say, $1 \ll N_t^{1/2} \ll M$. Note that if a given comb copolymer does not obey this relation, one may "scale up" the polymer until it does obey the relation since the upper bound grows linearly with the intertooth distance but the middle part of the inequality grows as the square root of the tooth length.

In the formulation of the random phase approximation (RPA) of Leibler¹ or the equivalent field theoretic version of Ohta and Kawasaki,² the connectivity of the system shows up only in the calculation of the Gaussian chain n -point connected correlation functions. The free energy of the system is calculated in terms of the monomer density of the A and B species, denoted by $\psi_A(\mathbf{r})$ and $\psi_B(\mathbf{r})$, respectively. The system is assumed to be incompressible and $\psi_A(\mathbf{r}) + \psi_B(\mathbf{r}) = \rho_0$. We will later set $\rho_0 = 1$.

The RPA mean-field free energy is determined as a functional expressed in powers of a field variable $\psi(\mathbf{r}) = f_B \psi_A(\mathbf{r}) - f_A \psi_B(\mathbf{r})$. The interaction between the monomers reduces to

$$-\chi \int d^d r \psi^2(\mathbf{r}) \quad (1)$$

apart from a constant, assuming a δ function interaction between monomers on the chains. In the RPA, the free energy for a given ψ configuration is calculated using a saddle point approximation.² The resulting free energy is then expanded in powers of ψ . At the end, one is left to calculate $S(\mathbf{q})$, where $S^{-1}(\mathbf{q}) = \Gamma_2(\mathbf{q})$ is the two-point vertex function in the RPA free energy. If $S(\mathbf{q})$ diverges for some $|\mathbf{q}| > 0$, that is $\Gamma_2 \rightarrow 0$, it signals a finite wavelength thermodynamic instability, a characteristic of microphase separation.

Now, $S(\mathbf{q})$ has the form

$$S(\mathbf{q}) = \frac{W(\mathbf{q})}{T(\mathbf{q}) - 2\chi W(\mathbf{q})} \quad (2)$$

where $W(\mathbf{q})$ and $T(\mathbf{q})$ are defined in terms of the two-point Gaussian chain correlation functions between A and B type monomers as follows:

$$\begin{aligned} W(\mathbf{q}) &= S_{AA}(\mathbf{q}) S_{BB}(\mathbf{q}) - S_{AB}^2(\mathbf{q}) \\ T(\mathbf{q}) &= S_{AA}(\mathbf{q}) + S_{BB}(\mathbf{q}) + 2S_{AB}(\mathbf{q}) \end{aligned} \quad (3)$$

with the density-density correlation functions between monomers of type α and β given by $S_{\alpha\beta}(\mathbf{q}) = \langle \psi_\alpha(-\mathbf{q}) \psi_\beta(\mathbf{q}) \rangle_0$. The $\langle \dots \rangle_0$ represents averages over the noninteracting Gaussian chain Hamiltonian with connectivity constraints.

The calculation of $S_{\alpha\beta}(\mathbf{q})$ is based upon the integration over a subset of monomers of the intrapolymer monomer-monomer correlation function. Written in real space, this is

$$S_{\alpha\beta}(\mathbf{r}-\mathbf{r}') = \sum_{\substack{j \in \alpha \\ j' \in \beta}} \int_0^{N_j} d\tau \int_0^{N_{j'}} d\tau' \frac{c}{n} \sum_{i=1}^n \langle \delta(\mathbf{r}_i^j(\tau) - \mathbf{r}) \times \\ \delta(\mathbf{r}_i^{j'}(\tau') - \mathbf{r}') \rangle_0 \quad (4)$$

where n is the number of comb polymers in the system and $c \equiv n/V$ is the polymer number density. Also i indexes each polymer, j and j' indicate the subchain in a single polymer, where $j \in \alpha$ denotes the restriction to subchains of monomer type α , and τ is the monomeric coordinate along a subchain j .

This, in turn, is simplified by realizing that the non-interacting flexible comb polymer behaves like a linear Gaussian chain segment between any two points on the polymer, irrespective of being on a tooth or backbone, since the chain is acyclic. We assume that monomer size is constant between the different species. We use the fact that the probability for ends of a Gaussian chain segment of M monomers to be at \mathbf{r} and \mathbf{r}' is governed, as usual, by

$$P(\mathbf{r}, \mathbf{r}', M) \propto \exp\left(\frac{-3(\mathbf{r} - \mathbf{r}')^2}{2b^2M}\right) \quad (5)$$

where b is essentially the unit monomer length.⁸ Multi-point monomer correlation functions for the comb are more complex than in the linear copolymer case since, generally, arbitrary sets of monomers do not lie on a single line over the entire polymer.

Using the above, one finds for the evenly spaced case that

$$S_{AA}(\mathbf{q}) = cN^2 \int_0^{f_A} d\tau \int_0^{f_A} d\tau' \exp(-q^2 R^2 |\tau - \tau'|) \\ S_{BB}(\mathbf{q}) = cN^2 n_t \int_0^{f_{Bt}} d\tau \int_0^{f_{Bt}} d\tau' \exp(-q^2 R^2 |\tau - \tau'|) + \\ cN^2 \sum_{\substack{i,j=1 \\ i \neq j}}^{n_t} \int_0^{f_{Bt}} d\tau \int_0^{f_{Bt}} d\tau' \exp(-q^2 R^2 (\tau + \tau' + f_{Ad} |i - j|)) \\ S_{AB}(\mathbf{q}) = cN^2 \sum_{i=1}^{n_t} \left[\int_0^{f_{At}(i-1+t)} d\tau \int_0^{f_{Bt}} d\tau' \exp(-q^2 R^2 (\tau + \tau')) + \right. \\ \left. \int_0^{f_{At}(n_t-i+1-t)} d\tau \int_0^{f_{Bt}} d\tau' \exp(-q^2 R^2 (\tau + \tau')) \right] \quad (6)$$

where $c \equiv n/V = \rho_0/N$ is the polymer number density (ρ_0 is the monomeric density) and $R^2 \equiv Nb^2/6$. In the following we let $\rho_0 = 1$, which sets $c = 1/N$. Fortunately, the above expressions for $S_{\alpha\beta}$ can be reduced to the following closed forms:

$$S_{AA}(\mathbf{q}) = \frac{2N}{(qR)^4} [e^{-f_A(qR)^2} + f_A(qR)^2 - 1]$$

$$S_{BB}(\mathbf{q}) = \frac{2Nn_t}{(qR)^4} [e^{-f_{Bt}(qR)^2} + f_{Bt}(qR)^2 - 1] +$$

$$\frac{2N}{(qR)^4} (e^{-f_{Bt}(qR)^2} - 1)^2 e^{-f_{At}(qR)^2} \left[\frac{n_t - 1 - e^{-(n_t-1)f_{At}(qR)^2}}{1 - e^{-f_{At}(qR)^2}} - \frac{e^{-f_{At}(qR)^2} (1 - e^{-(n_t-2)f_{At}(qR)^2})}{(1 - e^{-f_{At}(qR)^2})^2} \right]$$

$$S_{AB}(\mathbf{q}) = \frac{N}{(qR)^4} (e^{-f_{Bt}(qR)^2} - 1) \left(-2n_t + (e^{-f_{At}(qR)^2} + e^{-(1-t)f_{At}(qR)^2}) \left(\frac{1 - e^{-n_t f_{At}(qR)^2}}{1 - e^{-f_{At}(qR)^2}} \right) \right) \quad (7)$$

The case with $t = 0$ was previously derived in ref 4 (see also ref 9).

Returning to eq 2, we now wish to find the minimum χ where $T(q) - 2\chi W(q) = 0$ is satisfied for some $q = q^*$. Fixing n_t and f_A , one notes that $S_{\alpha\beta}$ scales as N ; thus $T(q) \propto N$ and $W(q) \propto N^2$. This implies that the relevant parameter is actually (χN) . The spinodal condition can be written as

$$(\chi N)_s = \frac{NT(q^*)}{2W(q^*)} \quad (8)$$

The right-hand side is simply $(2S(q^*)/N)^{-1}$ at $\chi = 0$. To find $(\chi N)_s$ and q^* , one finds the maximum of $S(q)/N$ at $\chi = 0$. The value of q at the maximum is q^* , and $(\chi N)_s = N/2S(q^*)$.

In the case of the copolymer with randomly placed teeth, we must take into account the placement distribution of teeth. Here, we assume the simplest placement distribution. Each tooth is grafted onto the backbone at any point along the backbone with uniform probability. More realistic distributions should also be possible, along with varying the number of teeth on each polymer. However, we proceed with this simplest version of architectural dispersity. The basic difference between this case and the previous case is that the Gaussian chain correlation functions are averaged over an ensemble of copolymers with randomly placed teeth (see Appendix). $S_{AA}(\mathbf{q})$ is unchanged, but the other correlation functions become

$$S_{BB}(\mathbf{q}) = cN^2 n_t \int_0^{f_{Bt}} d\tau \int_0^{f_{Bt}} d\tau' \exp(-q^2 R^2 |\tau - \tau'|) + \\ cN^2 \int_0^1 dg^1 \int_0^1 dg^2 \dots \int_0^1 dg^{n_t} \\ \left[\sum_{i \neq j}^{n_t} \int_0^{f_{Bt}} d\tau \int_0^{f_{Bt}} d\tau' \exp(-q^2 R^2 (\tau + \tau' + f_A |g^i - g^j|)) \right] \quad (9) \\ S_{AB}(\mathbf{q}) = cN^2 \int_0^1 dg^1 \int_0^1 dg^2 \dots \int_0^1 dg^{n_t} \times \\ \left[\sum_{i=1}^{n_t} \left(\int_0^{g^i f_A} d\tau \int_0^{f_{Bt}} d\tau' \exp(-q^2 R^2 (\tau + \tau')) + \right. \right. \\ \left. \left. \int_0^{f_A(1-g^i)} d\tau \int_0^{f_{Bt}} d\tau' \exp(-q^2 R^2 (\tau + \tau')) \right) \right] \quad (10)$$

where g^i represents the relative attachment point of the i th tooth on the backbone. The above equations reduce to

$$S_{BB}(\mathbf{q}) = \frac{2Nn_t}{(qR)^4} [e^{-f_{Bt}(qR)^2} + f_{Bt}(qR)^2 - 1] + \\ \frac{2Nn_t(n_t - 1)}{f_A^2(qR)^8} (1 - e^{-f_{Bt}(qR)^2})^2 (f_A(qR)^2 + e^{-f_A(qR)^2} - 1) \quad (11)$$

$$S_{AB}(\mathbf{q}) = \frac{2Nn_t}{(qR)^6 f_A} (1 - e^{-f_{Bt}(qR)^2}) (f_A(qR)^2 + e^{-f_A(qR)^2} - 1) \quad (12)$$

With these equations, we can numerically determine the initial unstable wavelength and the spinodal curves.

III. Results and Discussion

In the following, we will redefine $Q = qR'$, where $R' = (b/6)(N/n_t)^{1/2}$. With this definition, the wave vector Q is

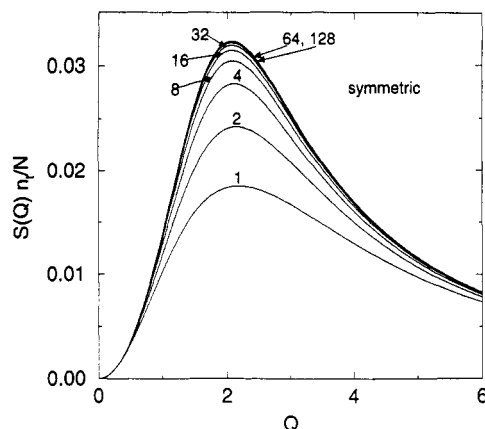


Figure 2. Plot of $(n_t/N)S(Q)$ as a function of Q at $\chi = 0$ for the symmetric, regularly spaced comb copolymer at $f_A = 0.2$ for various n_t , which are labeled on the curves.

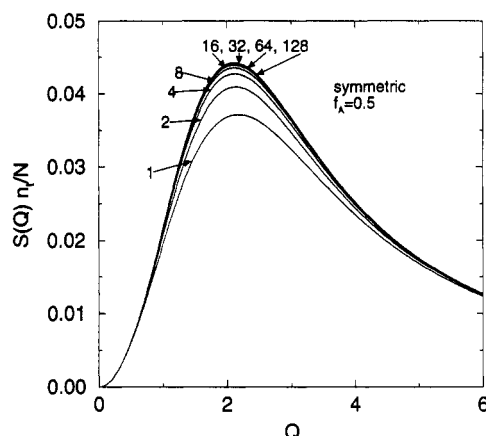


Figure 3. Plot of $(n_t/N)S(Q)$ as a function of Q at $\chi = 0$ for the symmetric, regularly spaced comb copolymer at $f_A = 0.5$ for various n_t , which are labeled on the curves.

measured roughly in units of the (inverse) radius of gyration of a polymer the size of a single tooth with its share of backbone. We will view the data in terms of fixed N/n_t while varying n_t , the number of teeth. This will emphasize the change in the phase behavior when one adds a tooth of fixed size along with its share of backbone as a unit. In the comb with randomly placed teeth, one is comparing the effect on the phase behavior of changing n_t , the number of teeth, but fixing N_B and f_A . Thus the backbone increases in size linearly with n_t .

First we examine the behavior of $S(Q)$ at $\chi = 0$ of the symmetric combs with evenly spaced teeth. Figures 2–4 show representative behavior of $S(Q)$ for different values of n_t for $f_A = 0.2, 0.5$, and 0.8 , respectively. Quite clearly, after about $n_t = 16$, the $S(Q)$ curves essentially reach an asymptotic, large- n_t form.

Figure 5 shows a plot of the spinodal curve, $(\chi N)_s/n_t$ versus f_A , for the symmetric, evenly spaced comb copolymer. The normalization with respect to n_t is chosen to account properly for the effect of changing the number of teeth, not simply increasing the polymer size. The main effect of increasing the number of teeth is to make the spinodal instability easier at small f_A .¹⁰ It is clear that beyond $n_t = 16$ the spinodal curves do not shift much, at least in the region of $0.1 \leq f_A \leq 0.9$. In fact, at large n_t the curves appear to reach a limiting form. Note that the minimum χ of the “limiting” spinodal curve is at about $f_A \approx 0.42$ in contrast to the minimum for the single-tooth case, which is at $f_A \approx 0.47$. This disparity due to the comb architecture is not as great as one might have expected.

Figure 6 shows the instability wave vector Q^* versus f_A . In general, Q^* is smaller at larger n_t , although the actual

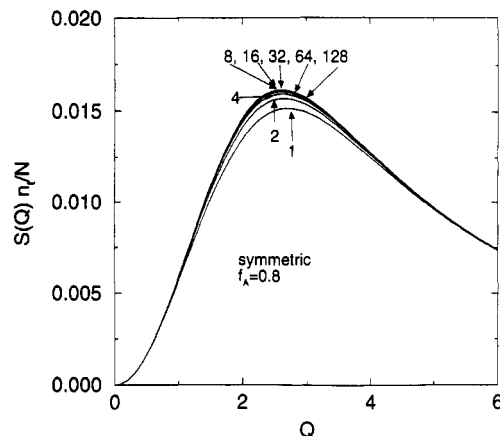


Figure 4. Plot of $(n_t/N)S(Q)$ as a function of Q at $\chi = 0$ for the symmetric, regularly spaced comb copolymer at $f_A = 0.8$ for various n_t , which are labeled on the curves. Note that for larger f_A , $S(Q)$ shows less variation in form with respect to n_t than for smaller f_A .

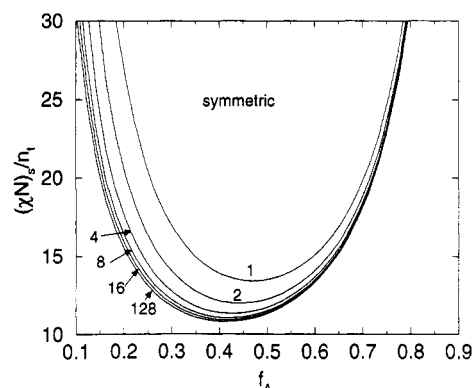


Figure 5. Plot of $(\chi N)_s/n_t$ as a function of f_A , the composition fraction of backbone “A” monomer. Note that the spinodal curve becomes more asymmetric about $f_A = 0.5$ as the number of teeth is increased. By ~ 16 teeth, the spinodal curve is practically fixed to the same form as the 128-tooth curve. After the tooth length and f_A are fixed, the system more easily microphase separates as more teeth are added.

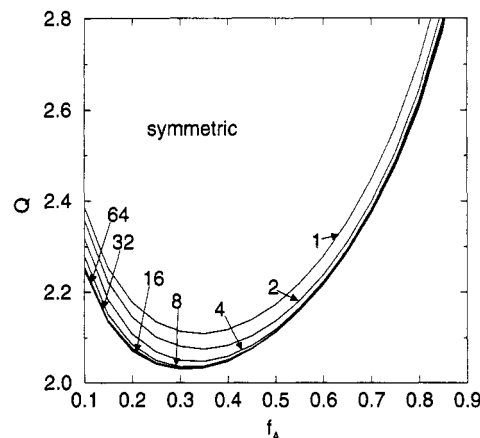


Figure 6. Plot of Q^* as a function of f_A for $n_t = 1, 2, 4, 8$, and 16 . The number of teeth increases from the upper line to the lower line in the plot. Note that the minimum Q^* is at $f_A = 0.32$ for $n_t = 16$. As the number of teeth increases and f_A increases, the Q^* plots nearly merge together. The dependence on n_t is most clear at smaller f_A .

change is relatively small. The minimum Q^* shifts from $f_A \approx 0.34$ for one tooth to $f_A \approx 0.31$ in the limit of large n_t . In this figure, and that of the spinodal curve (Figure 5), the effect of varying n_t is reduced at larger values of f_A .

However, the behavior of the spinodal curves as a function of the number of teeth, n_t , is quite different for the asymmetric case. As shown in Figure 7, only in the

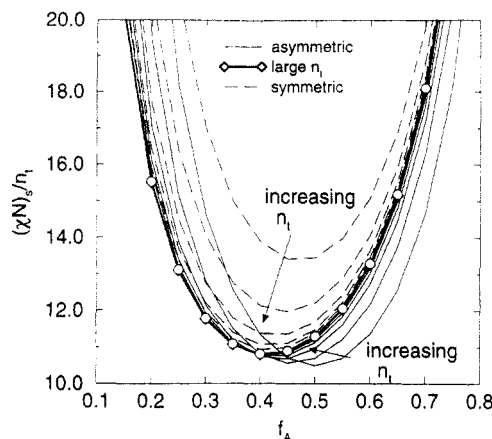


Figure 7. Plot of $(\chi N)/n_t$ as a function of f_A for asymmetric and symmetric combs for $n_t = 1, 2, 4, 8, 16$, and 128 . Note that the two systems converge to the same form at large n_t as expected. Also note that the approach to the large n_t curve is different and the curves are distinguishable for modest n_t .

large- n_t limit do the asymmetric curves collapse onto the same curve as the symmetric case. The asymmetric case approaches the fixed large- n_t form in a completely different fashion from that of the symmetric comb. Oddly, for the asymmetric case, the minimum χ actually rises as n_t increases, although only very slightly. This convergence to a fixed form, independent of the asymmetry, is not surprising since at large n_t , only the small region near the ends of the backbone is different. However, the fact that asymmetry has a noticeable effect at all for modest n_t suggests that random placement of teeth in a comb copolymer may produce important effects. To understand the difference in behavior for modest n_t , consider the case of just one tooth, or $n_t = 1$. In this example, we are clearly comparing the spinodal for a melt of diblocks (asymmetric case) with the spinodal for a melt of single-toothed combs (symmetric case). These copolymer melts clearly display different phase behaviors.

As stated previously, we studied an extreme case of uniformly random placement on the backbone of a fixed number of teeth. For the system with randomly placed teeth, we find that the behavior of $S(Q)$ is significantly different from that of the regularly spaced combs in that the $S(Q)$ curves do not settle down quickly into a large- n_t form. To help understand this behavior, we examine the $n_t \rightarrow \infty$ limit of $(n_t/N)S(Q)$ as a function of Q and f_A ,

$$\lim_{n_t \rightarrow \infty} \frac{n_t}{N} S(Q) = \frac{4f_A^2(e^{-Q^2(1-f_A)} + Q^2(1-f_A) - 1)}{\{1 - 2e^{-Q^2(1-f_A)} + e^{-2Q^2(1-f_A)} + (1 - e^{-Q^2(1-f_A)})Q^2f_A + Q^4f_A\}} \quad (13)$$

Figures 8–10 show $S(Q)$ at $\chi = 0$ for the random comb system for $f_A = 0.2, 0.5$, and 0.8 , respectively. In contrast to the evenly spaced combs, the $S(Q)$ curves do not settle down to the large- n_t form very quickly. For f_A less than ~ 0.5 , it appears that $S(Q)$ has a definite maximum at finite Q in the large- n_t limit. Curiously, the $S(Q)$ curve has significant amplitude even for $Q < Q^*$. However, for f_A greater than ~ 0.5 it appears that $S(Q)$ has a maximum at $Q = 0$ in the limit $n_t \rightarrow \infty$. Empirically rescaling the Q axis, as shown for $f_A = 0.8$ in Figure 11, by $Qn_t^{1/4}$ reveals that the peaks of $S(Q)$ appear to line up for large n_t , although the $S(Q)$ curves themselves continue to broaden. This suggests that above $f_A \approx 0.5$, the scaling of the characteristic wavelength with respect to n_t is altered.

The effect of this dispersity on $(\chi N)/n_t$ versus f_A is shown in Figure 12. As n_t is increased, the minimum of

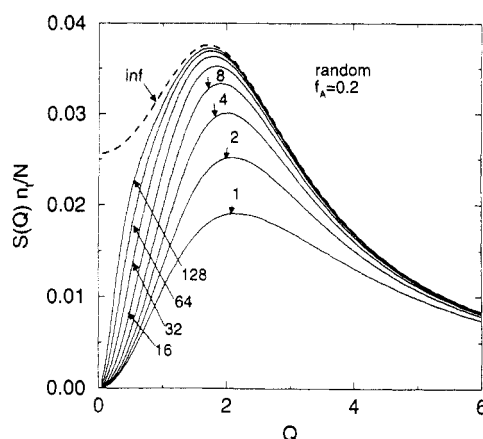


Figure 8. $(n_t/N)S(Q)$ as a function of Q at $\chi = 0$ for the randomly spaced comb copolymer at $f_A = 0.2$ for various n_t . The curve labeled "inf" is $S(Q)$ in the limit $n_t \rightarrow \infty$. Note that in this limit $S(Q)$ does have a maximum at finite Q .

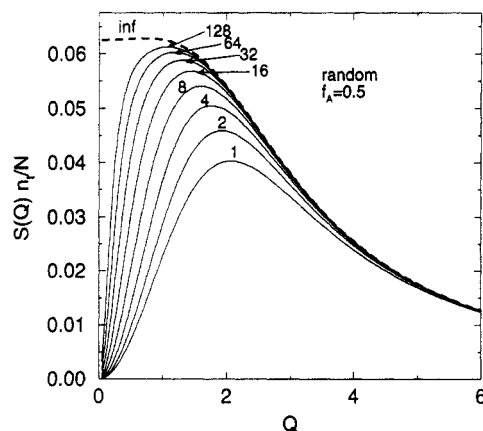


Figure 9. $(n_t/N)S(Q)$ as a function of Q at $\chi = 0$ for the random comb copolymer at $f_A = 0.5$ for various n_t . The maximum of $S(Q)$ as $n_t \rightarrow \infty$ is barely discernible.

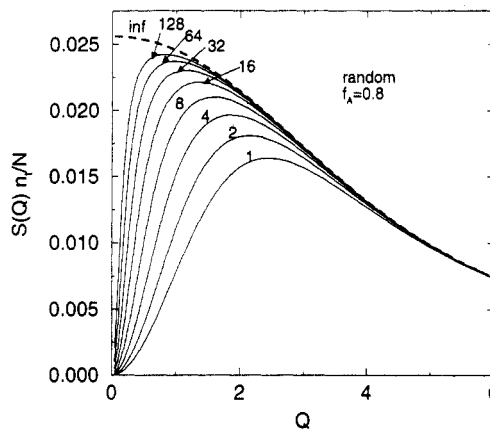


Figure 10. $(n_t/N)S(Q)$ as a function of Q at $\chi = 0$ for the random comb copolymer at $f_A = 0.8$ for various n_t . Note that in the limit $n_t \rightarrow \infty$ $S(Q)$ does not have a maximum at $Q > 0$.

spinodal curves shifts slightly toward smaller values. Clearly, the $(\chi N)_s$ curves for the randomly spaced comb copolymer are very different from those for the regularly spaced comb copolymer, although the minimum is located at f_A slightly smaller than 0.5 as in the regular case. The χN curve does not settle quickly into a large- n_t form as in the regular comb case.

To examine further the characteristic length scales in the random case, we plot Q^* , the characteristic wave vector of the random comb, in Figure 13. As n_t is increased, the minimum Q^* shifts to higher f_A . In contrast to the regular

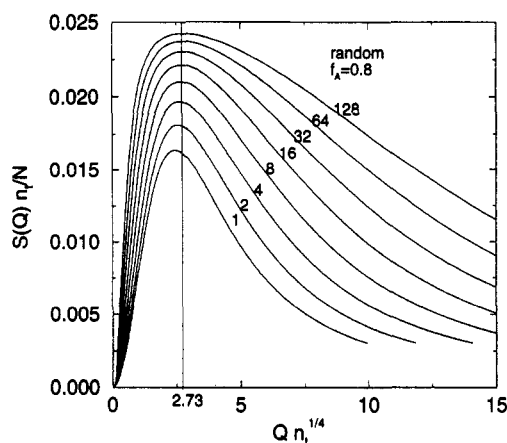


Figure 11. $(n_t/N)S(Q)$ as a function of $Q n_t^{1/4}$ at $\chi = 0$ for the random comb copolymer at $f_A = 0.8$ for various n_t . Under this rescaling, the peak of $S(Q)$ appears to be at a nonzero value of Q in the limit of large n_t . This would suggest a qualitatively different microphase separation behavior than for the smaller f_A cases.

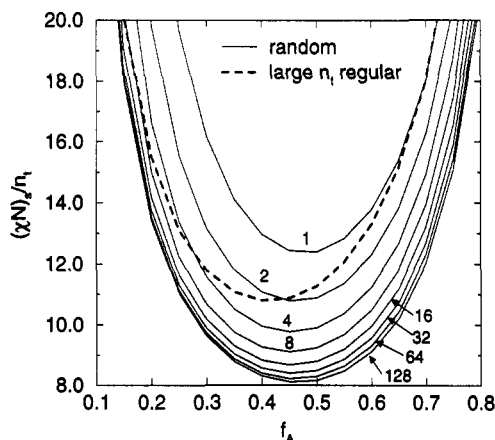


Figure 12. $(\chi N)/n_t$ as a function of f_A for combs with randomly placed teeth versus the large- n_t form of the spinodal curve of the regularly spaced combs. Randomness lowers the minimum of the spinodal curve at large n_t . The large- n_t curves for the regular and random systems are very different.

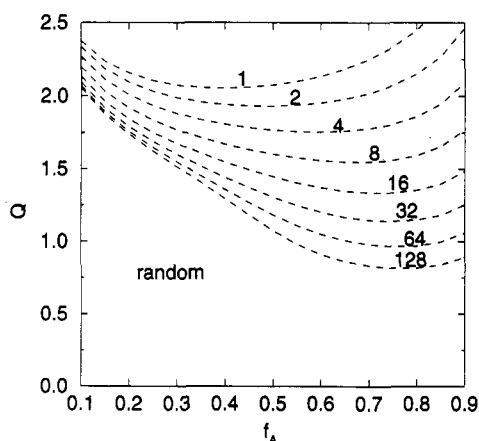


Figure 13. Q^* as a function of f_A for the comb copolymer with randomly placed teeth.

comb system where the minimum Q^* occurs at about $f_A \approx 0.31$ in the large- n_t limit, the minimum for the random comb is at $f_A > 0.7$ even at $n_t = 16$. Interestingly, the Q^* curve is no longer concave beyond $n_t = 128$. In Figure 14, we plot Q^* as calculated from the limit $n_t \rightarrow \infty$. Clearly, there is a kind of "critical point" for Q^* at $f_A = f_{Ac} \approx 0.543$. For $f_A \leq f_{Ac}$ one finds that $Q^* \sim (f_{Ac} - f_A)^{1/2}$. For $f_A > f_{Ac}$ we expect that Q^* scales like $n_t^{-1/4}$ as we demonstrated previously in Figure 11. We take this to indicate that there exist for $f_A > f_{Ac}$ large (on the scale of a single tooth)

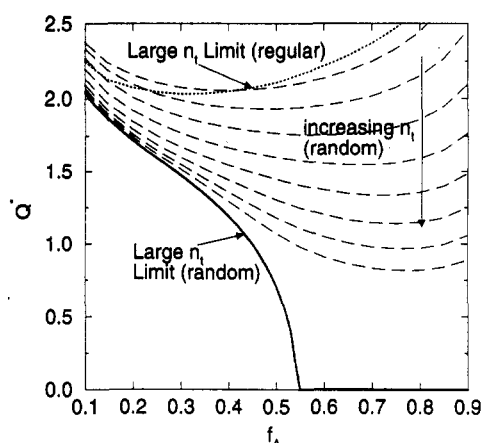


Figure 14. Q^* as a function of f_A for the combs with randomly placed teeth and combs with regularly spaced teeth. The minimum point of the curves are at completely different f_A . Further, the random combs at large n_t have a very small minimum Q^* . The $n_t \rightarrow \infty$ curve shows a clear singular behavior around $f_A = f_{Ac} \approx 0.543$. The behavior is reminiscent of a kind of critical point, and $Q^* \sim (f_{Ac} - f_A)^{0.50}$ for $f_A < f_{Ac}$.

relatively bare regions of backbone which microphase separate at lengths greater than the radius of gyration of a single-tooth unit. Rewriting this using the physical q , we see that this implies for $f_A < f_{Ac}$ $q^* \sim (n_t/N)^{1/2}$ for large n_t as expected. However, for $f_A > f_{Ac}$, $q^* \sim n_t^{1/4}/N^{1/2}$, which is not expected.

We finish with a note concerning the possibility of a mean-field critical point. In general, to compute the existence of a critical point, one must also consider the third-order vertex function, Γ_3 .¹ It is generally noted that for architectures such as a diblock,¹ triblock, and star copolymer¹¹ for $f \rightarrow 0$, $\Gamma_3(q^*) < 0$ and for $f \rightarrow 1$, $\Gamma_3(q^*) > 0$. One may expect the same result to hold in the comb case because, in the limits indicated, the architecture is essentially the same as one of the above examples. This implies that at some f , between 0 and 1, $\Gamma_3 = 0$ assuming it is continuous in f . This further implies that a mean-field critical point exists at some f_c . Without the symmetry of the diblock case, the exact f_c must be explicitly calculated.

IV. Summary

In this paper, we have investigated the effect of architecture on the phase behavior of copolymer combs. Even a simple adjustment of architecture from asymmetric to symmetric evenly spaced teeth causes a change in the form of the $(\chi N)_s$ as a function of f_A , particularly at modest numbers of teeth. The two systems converge in behavior as n_t gets larger, as expected.

However, when the tooth placement on the backbone is allowed to be random, the spinodal curve is significantly different from that of the evenly spaced cases. In addition, the behavior of the characteristic wavelength as a function of f_A is drastically different between the randomly and evenly spaced cases. One expects that more complete calculations, for example of third- and fourth-order terms in the free energy in the weak-segregation regime, would allow one to observe significant changes in the equilibrium morphology of the systems due to random placement of teeth. The essential point is that a correct description of architectural dispersity is important and can lead to significant changes in phase behavior from the ideal cases usually studied. This architectural dispersity is an additional issue to that of the effects of ordinary polydispersity in the size of the polymers.

Acknowledgment. A.S. and A.C.B. gratefully acknowledge helpful discussions with Eugene Gurovich. The

work is, in part, supported by the National Science Foundation (Grants NSF-DMR-92-17935 and NSF-DMR-91-07102).

Appendix

In general, to deal with quenched randomness, one must perform an average over the randomness after the free energy is computed for each given instance of the randomness. In our case the randomness involves the points where the teeth are attached to the backbone.

Let \mathbf{g}_i represent a vector of n_t elements ($g_i^1, g_i^2, \dots, g_i^{n_t}$). Each element g_i^m obeys $0 \leq g_i^m \leq 1$ and denotes the relative position on the backbone of the m th tooth of the i th polymer. In general, there is some probability measure associated with \mathbf{g}_i which we will call μ_g . In the simple picture we used in the paper

$$\mu_g(\mathbf{g}_i) = \prod_{m=1}^{n_t} \mu_0(g_i^m) \quad (14)$$

where μ_0 is the uniform probability over the interval $[0,1]$. However, nothing prevents the use of an alternative, perhaps more realistic, μ_g .

Let \mathbf{G} represent the sequence ($\mathbf{g}_1, \mathbf{g}_2, \dots, \mathbf{g}_n$), where n is the number of polymers in the system. In the thermodynamic limit, $n \rightarrow \infty$. There is also a measure induced for \mathbf{G} itself: $\mu\{\mathbf{G}\} = \prod_i \mu_g(\mathbf{g}_i)$. We must first calculate the free energy, or correlation function, for our system for a realization of \mathbf{G} and then average over \mathbf{G} . This amounts to

$$S(\mathbf{q}) = \int d\mu\{\mathbf{G}\} \frac{\delta F[h, \mathbf{G}]}{\delta h(\mathbf{q}) \delta h(-\mathbf{q})} = \int d\mu\{\mathbf{G}\} S(\mathbf{q}; \mathbf{G}) \quad (15)$$

where $F[h, \mathbf{G}]$ is the free energy of the system for a given instance of \mathbf{G} and $h(\mathbf{q})$ is a field coupling linearly with ψ . In mean-field theory, we can evaluate in principle $S(\mathbf{q}; \mathbf{G})$. This gives us the usual

$$S(\mathbf{q}; \mathbf{G}) = \frac{W(\mathbf{q}; \mathbf{G})}{T(\mathbf{q}; \mathbf{G}) - 2\chi W(\mathbf{q}; \mathbf{G})}$$

$$W(\mathbf{q}; \mathbf{G}) = S_{AA}(\mathbf{q}; \mathbf{G}) S_{BB}(\mathbf{q}; \mathbf{G}) - S_{AB}^2(\mathbf{q}; \mathbf{G})$$

$$T(\mathbf{q}; \mathbf{G}) = S_{AA}(\mathbf{q}; \mathbf{G}) + S_{BB}(\mathbf{q}; \mathbf{G}) + 2S_{AB}^2(\mathbf{q}; \mathbf{G}) \quad (16)$$

However,

$$S_{\alpha\beta}(\mathbf{q}; \mathbf{G}) = \frac{1}{n} \sum_{i=1}^n s_{\alpha\beta}(\mathbf{q}; \mathbf{g}_i) \quad (17)$$

where $s_{\alpha\beta}(\mathbf{q}; \mathbf{g}_i)$ are the single-polymer correlation functions between monomers of type α and β for a given architecture \mathbf{g}_i . Note that $s_{\alpha\beta}(\mathbf{q}; \mathbf{g}_i)$ is a bounded function of \mathbf{g}_i . In the limit $n \rightarrow \infty$, one can use the strong law of large numbers¹² and realize that with probability 1 with respect to the measure μ that

$$S_{\alpha\beta}(\mathbf{q}; \mathbf{G}) = S_{\alpha\beta}^{\text{avg}}(\mathbf{q}) \equiv \int d\mu_g(\mathbf{g}) s_{\alpha\beta}(\mathbf{q}; \mathbf{g}) \quad (18)$$

We then arrive at the averaging procedure used in this paper.

References and Notes

- (1) Leibler, L. *Macromolecules* **1980**, *13*, 1602.
- (2) Ohta, T.; Kawasaki, K. *Macromolecules* **1986**, *19*, 2621.
- (3) Olvera de la Cruz, M.; Sanchez, I. C. *Macromolecules* **1986**, *19*, 2501.
- (4) Benoit, H.; Hadziioannou, G. *Macromolecules* **1988**, *21*, 1449.
- (5) Fredrickson, G.; Helfand, E. *J. Chem. Phys.* **1987**, *87*, 697.
- (6) Mayes, A. M.; Olvera de la Cruz, M. *J. Chem. Phys.* **1991**, *95*, 4670.
- (7) Olmsted, P. D.; Milner, S. T., preprint (1993).
- (8) Doi, M.; Edwards, S. F. *The Theory of Polymer Dynamics* (Vol. 73 of *International Series of Monographs on Physics*); Oxford University Press: Oxford, 1988.
- (9) Dobrynin, A. V.; Erukhimovich, I. Y. *Macromolecules* **1993**, *26*, 276.
- (10) The general change of the spinodal curves with increasing teeth are reminiscent of a similar effect in a system of $(AB)_n$ star copolymers³ with increasing number n of (AB) arms. However, the effect is less dramatic in combs. In the star, the existence of a single junction point which concentrates the A side of the (AB) branch appears to induce self-micellarization.
- (11) Mayes, A. M.; Olvera de la Cruz, M. *J. Chem. Phys.* **1989**, *91*, 7228.
- (12) Doob, J. L. *Stochastic Processes*; Wiley: New York, 1953.